

Assessing the Radiometric Consistency between S-NPP VIIRS and NOAA-19 AVHRR for Data Continuity

Sirish Uprety^a, Changyong Cao^b

CIRA, Colorado State University^a, NOAA/NESIDS/STAR^b

Outline

- Objective
- Introduction
- S-NPP VIIRS and NOAA-19 AVHRR inter-comparison
 - SNO/SNO-x
 - Instruments
 - Methodology
 - Results and Analysis
- Summary and future work

Objective

- Assess the radiometric consistency between Suomi NPP VIIRS and NOAA-19 AVHRR over visible ($0.64 \mu\text{m}$) and near-infrared ($0.86 \mu\text{m}$) bands for Data Continuity
 - Analyze radiometric performance of NOAA-19 AVHRR by using SNOs in polar region and extended low latitude SNOs.
 - Use Dome C site to for validation.

Introduction

- Post-launch Sensor calibration/validation
 - Onboard calibrators
 - Vicarious sites such as desert, ocean, snow etc.
 - Exo-terrestrial targets such as moon, stars etc.
 - Inter-calibration with other instruments (SNO/SNO-x, desert targets etc).
- NOAA series AVHRR instruments lacks OBC system.
- AVHRR relies on desert (21° - 23° N, 28° - 29° E) for on-orbit relative calibration.
- Radiometric performance of AVHRR can be independently evaluated by performing inter-comparison with well calibrated radiometers such as VIIRS, MODIS etc.
- This study focus on comparing VIIRS with N-19 AVHRR VNIR bands in an effort to evaluate the radiometric consistency.
 - establish data continuity to multi-decadal Earth observation
 - Useful to detect and study the long term global changes such as climate change study, landcover/landmass change etc.

SNO and SNO-x

- Simultaneous nadir overpass (*SNO*): Comparison of simultaneous measurements between two or more instruments at their orbital intersection with nearly identical viewing conditions.
- SNOs usually occur at high-latitude polar region for polar orbiting satellites.
- However, there exists SNO events between Suomi NPP and NOAA-19 at low latitudes, but with larger time differences of more than 10 minutes.
- *SNO-x* in low latitudes is an approach inherited from traditional SNO approach that extends SNO orbits to low latitudes for inter-comparing sensors over a wide dynamic range such as over ocean surface, desert targets, green vegetation etc.
- In this study, VIIRS and AVHRR sensors are compared at overlapping regions of extended SNO orbits at North African deserts.



Instruments used in the Study

- **VIIRS**
 - Sun-synchronous polar orbiting instrument launched in October 2011 with full global coverage of Earth twice daily from an altitude of 829 km
 - Multispectral scanning radiometer with 16 moderate resolution bands (0.4 μm to 12 μm), 5 Imagery bands (0.6 μm to 12 μm) and 1 day night band (DNB).
 - Wide-swath (3,000 km) scanning radiometer with spatial resolution: 750m for moderate resolution bands and DNB , 375 m for imagery bands.
 - Equipped with solar diffuser (SD) and black body as onboard calibrators
- **AVHRR**
 - Launched aboard NOAA and MetOp series of meteorological satellites
 - first 2 bands (0.64 μm and 0.86 μm) of the AVHRR closely match with the VIIRS (M-5 and M-7) reflective solar bands
 - No onboard calibrators for solar reflective bands
 - Uses desert target (21°- 23° N, 28°- 29° E) for post launch on-orbit calibration
- **EO-1 Hyperion**
 - Push broom hyper-spectral sensor with 220 spectral bands ranging from 0.4 μm to 2.5 μm
 - Footprint size of 30m and spectral resolution of ~ 10 nm.
 - The radiometric calibration/validation is monitored using solar, lunar and in-flight calibration sources

Methodology

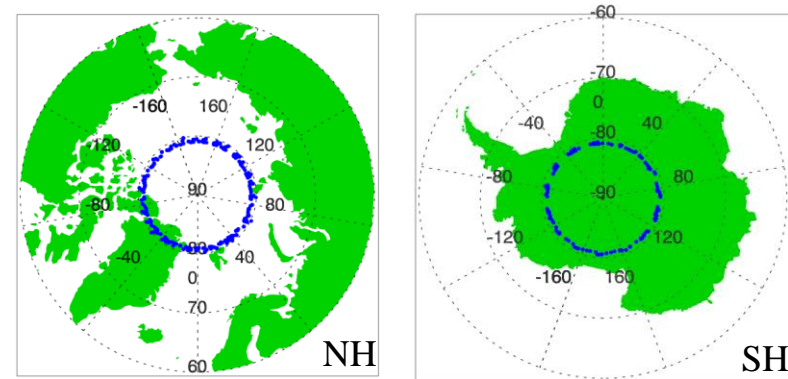
SNO

- For each SNO event, download VIIRS and N-19 AVHRR GAC data
- Extract ROI (20km * 20km) of VIIRS and AVHRR with center @ orbital intersection
- Calculate mean of all pixels within ROI
- Bias= $(VIIRS-AVHRR)*100\%/VIIRS$
- Repeat above steps for all SNO events and extract bias time series

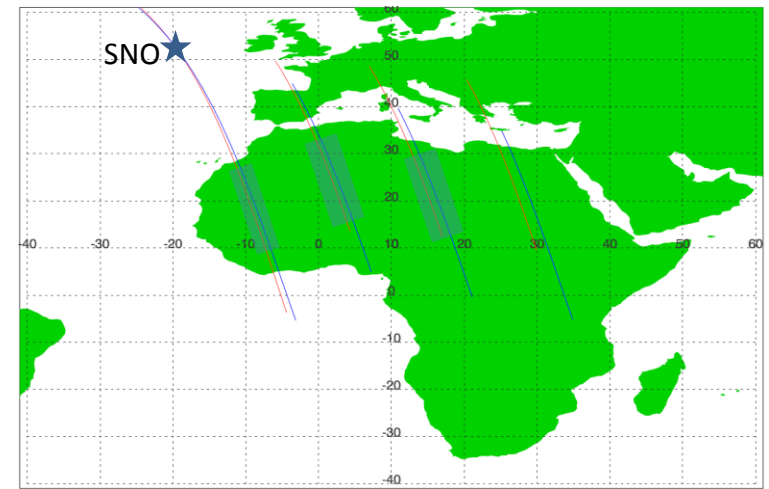
SNO-x

- For each SNO-x event, download VIIRS and N-19 AVHRR GAC data
- Find overlapping region in the desert
- Extract multiple collocated ROIs (20km * 20km) of VIIRS and AVHRR
- Calculate mean of all pixels within each ROI
- Bias= $(VIIRS-AVHRR)*100\%/VIIRS$
- Calculate mean and stdev of all biases for each SNO-x event
- Extract bias time series and analyze AVHRR rad. performance

SNO



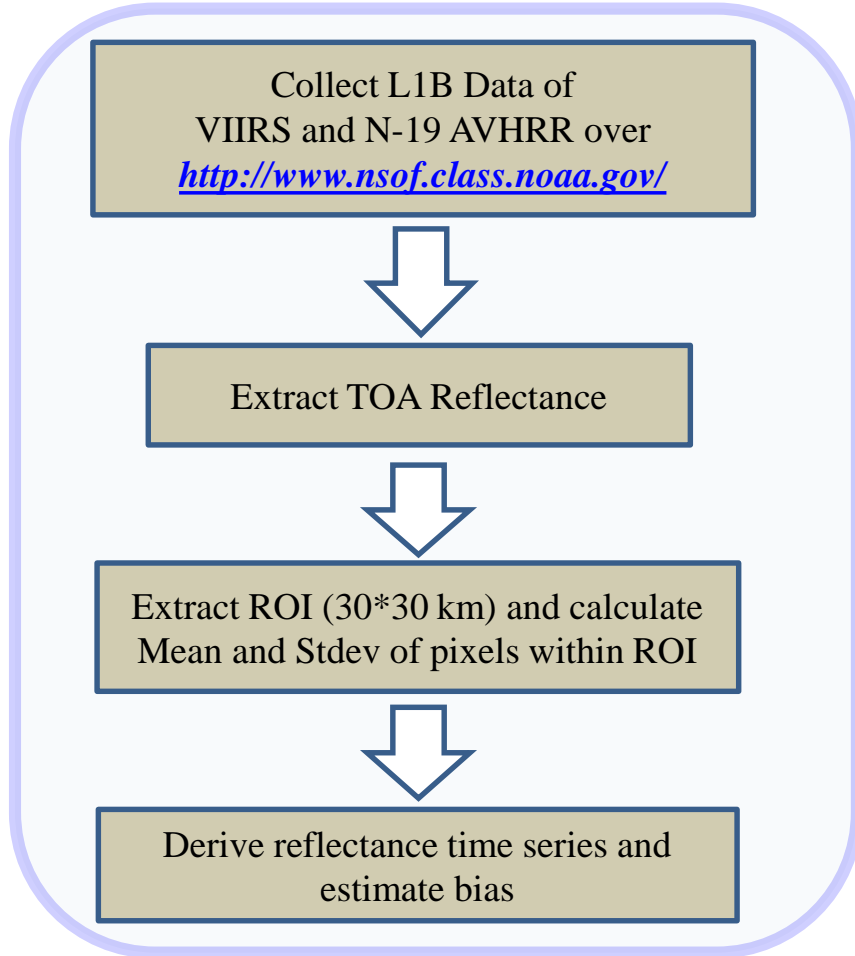
SNO-x



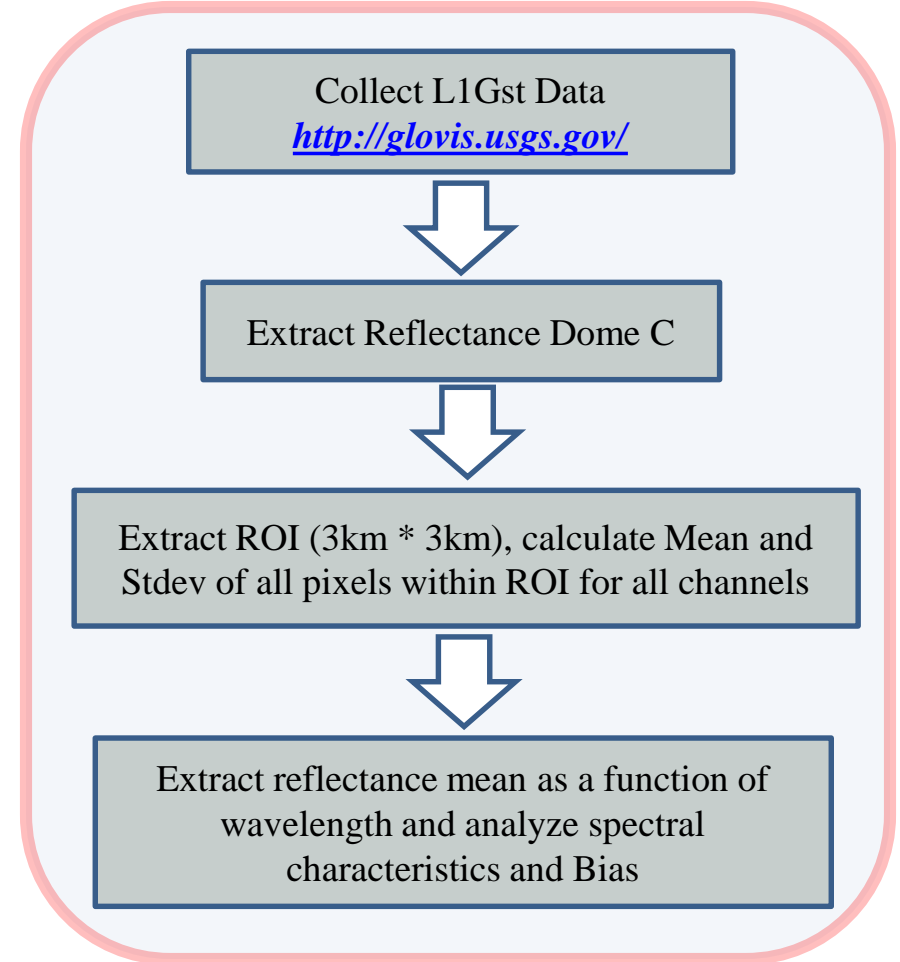
Note: Time Difference for SNO: <90 seconds and SNO-x: <20 mins.

Methodology

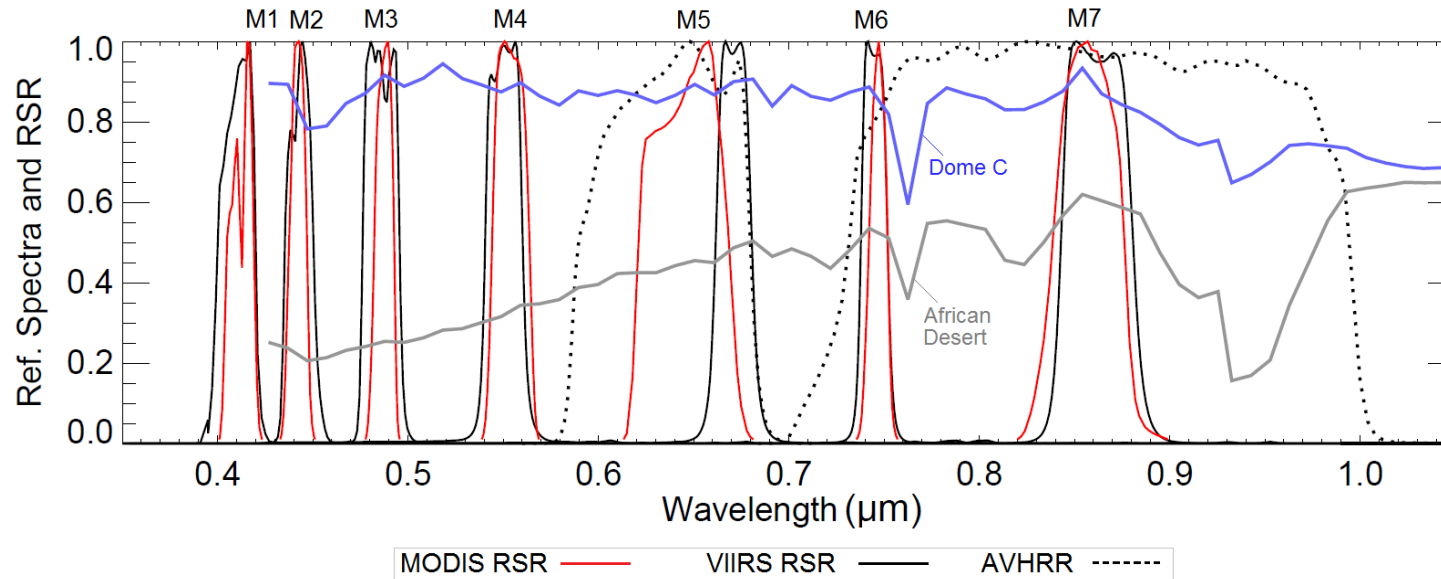
Dome C: TOA Ref. time series



EO-1 Hyperion: Hyperspectral analysis



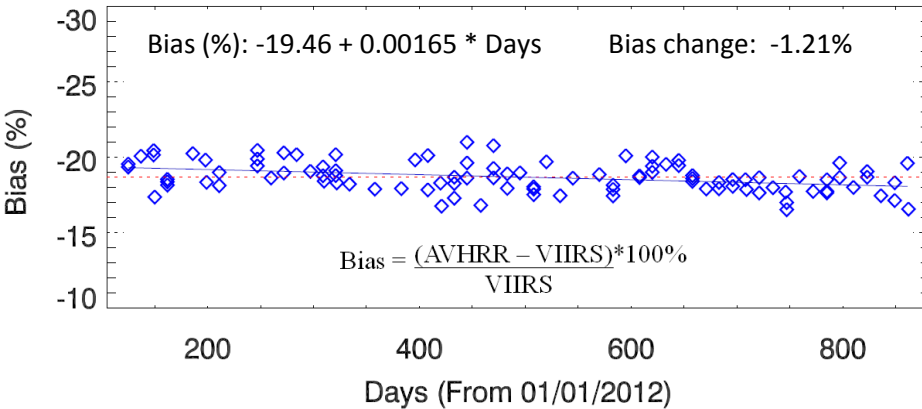
VIIRS, MODIS and AVHRR Matching Bands



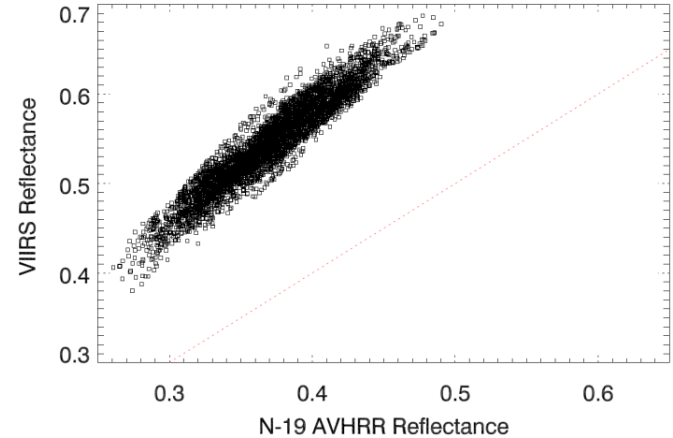
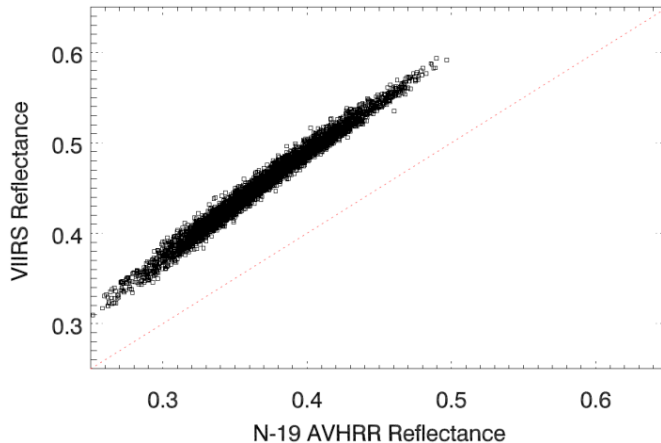
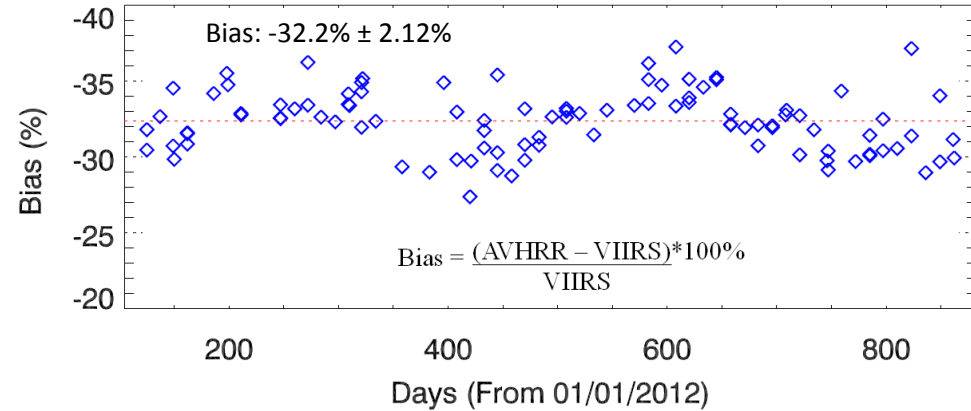
VIIRS		MODIS		AVHRR	
Band	Wavelength (μm)	Band	Wavelength (μm)	Band	Wavelength (μm)
M1	0.402 - 0.422	8	0.405 - 0.420	-	-
M2	0.436 - 0.454	9	0.438 - 0.448		
M3	0.478 - 0.498	10	0.483 - 0.493		
M4	0.545 - 0.565	4	0.545 - 0.565		
M5	0.662 - 0.682	1	0.620 - 0.670	1	0.58 - 0.68
		13	0.662 - 0.672		
M6	0.739 - 0.754	15	0.743 - 0.753	-	-
M7	0.846 - 0.885	2	0.841 - 0.876	2	0.725 - 1.0
		16	0.862 - 0.877		
M8	1.230 - 1.250	5	1.230 - 1.250	-	-

SNO-x Results (Desert)

AVHRR Band1 (0.64 μm) and VIIRS Band M-5



AVHRR Band 2 (0.86 μm) and VIIRS Band M-7

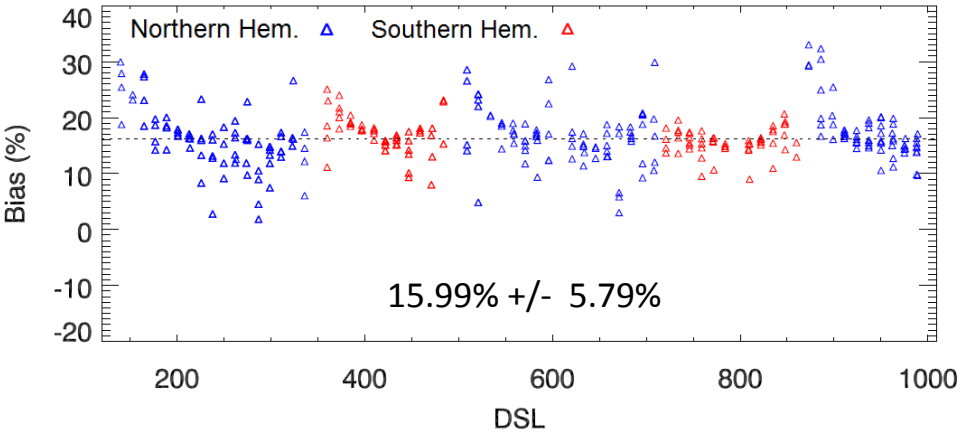


- Figure indicates AVHRR B1 degradation by about 1.2% over the period of 2 years.
- Number SNO-x events used, M5: 83 M8: 88

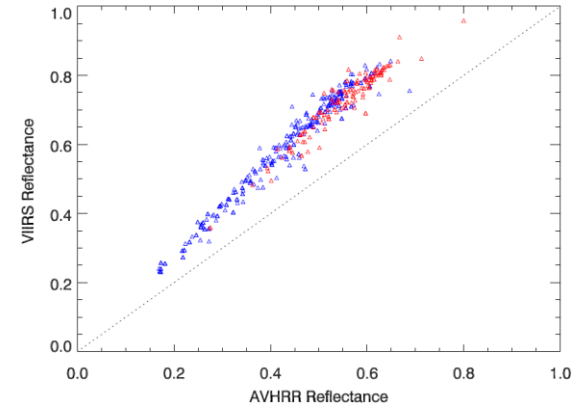
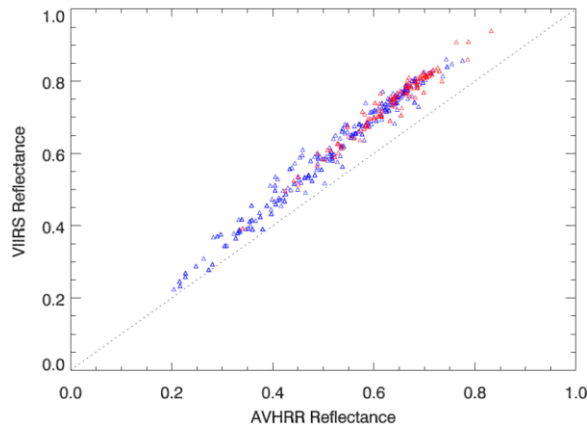
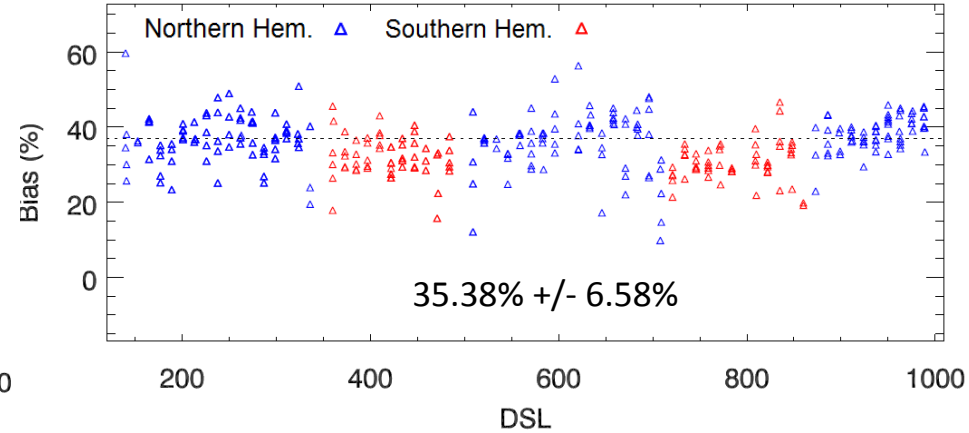
Note: AVHRR data used is post-launch calibrated data.

SNO Results

AVHRR Band1 (0.64 μm) and VIIRS Band M-5

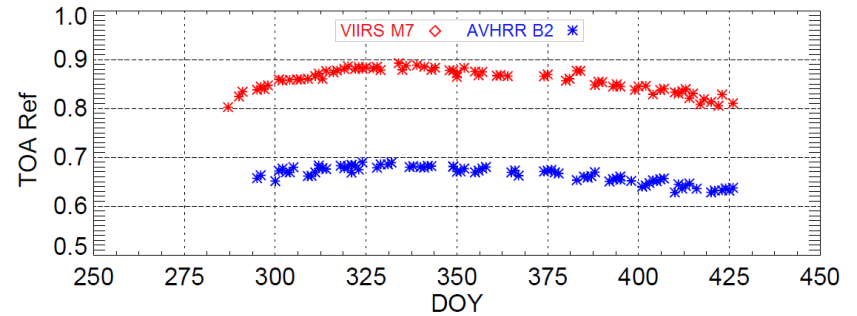
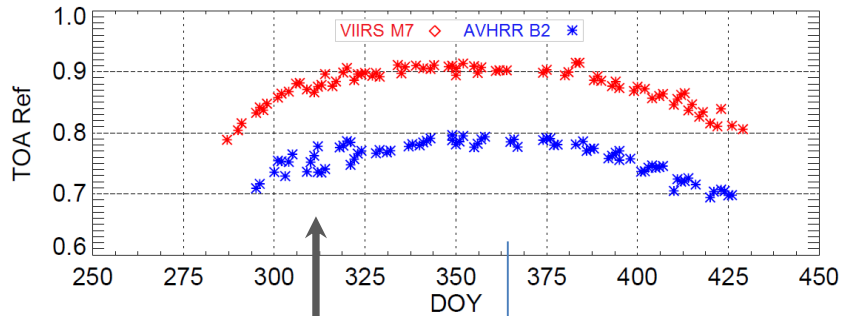
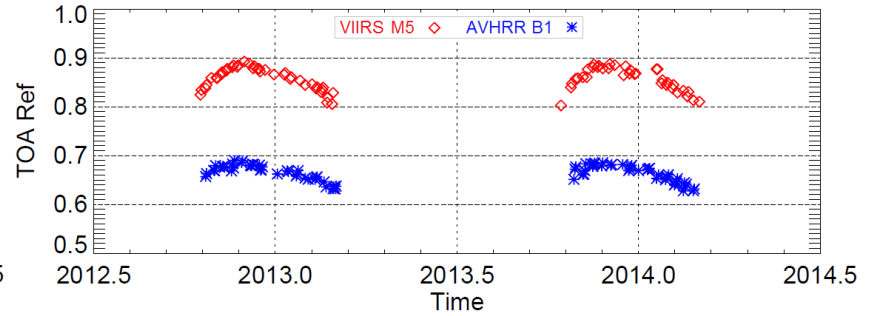
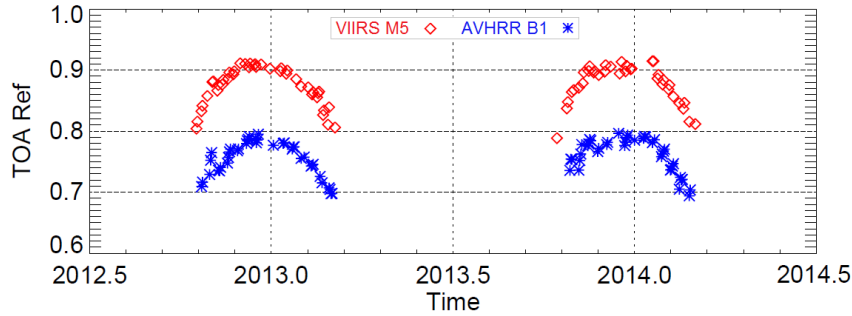


AVHRR Band 2 (0.86 μm) and VIIRS Band M-7



- Larger variability in NH for AVHRR B1 due to target variability compared to mostly snow over SH.
- AVHRR B2 bias indicates large water vapor absorption variability.
- Bias is mainly due to calibration uncertainty, spectral differences, and atmospheric variability. 11

Comparison over Dome C



Large variability \rightarrow $DOY = DOY (Jan-Mar) + 365 \text{ or } 366$

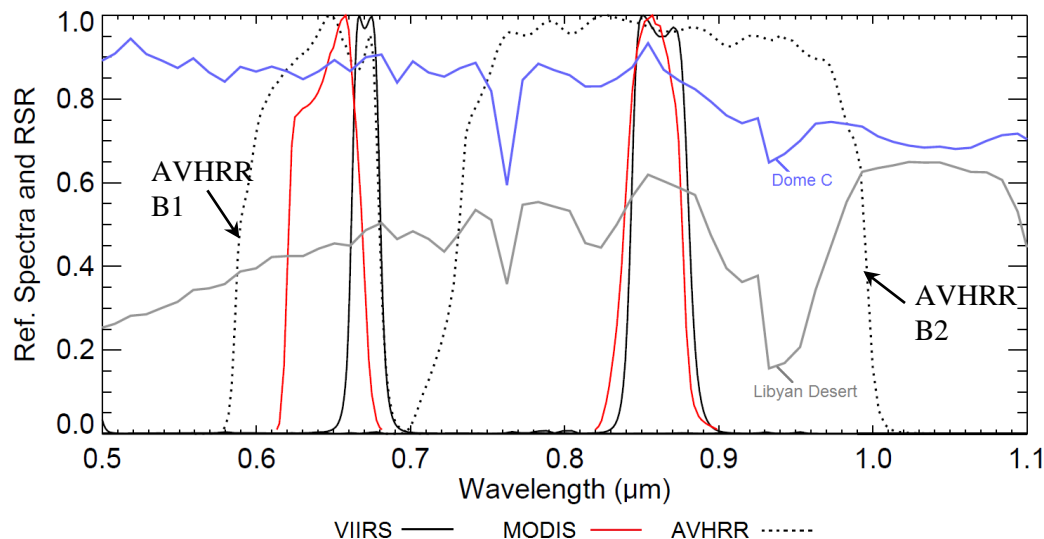
Note: AVHRR B1 suggest larger scatter during Oct-Dec mainly due to ozone absorption variability at nearly 0.6 μm .

AVHRR (μm)	VIIRS (μm)	AVHRR Observed Bias (DOY = 340)
B1 (0.58 – 0.68)	M5 (0.662 - 0.682)	-13.05% \pm 0.83%
B1 (0.725 – 1.0)	M7 (0.846 - 0.885)	-22.5% \pm 0.71%

Expected Spectral Bias

- Expected Spectral Bias (ESB) exists due to differences in RSR shape and spectral coverage between AVHRR and VIIRS bands.
 - simulated reflectance for VIIRS and AVHRR is estimated by convolving hyperspectral measurements of North African desert with instrument RSRs

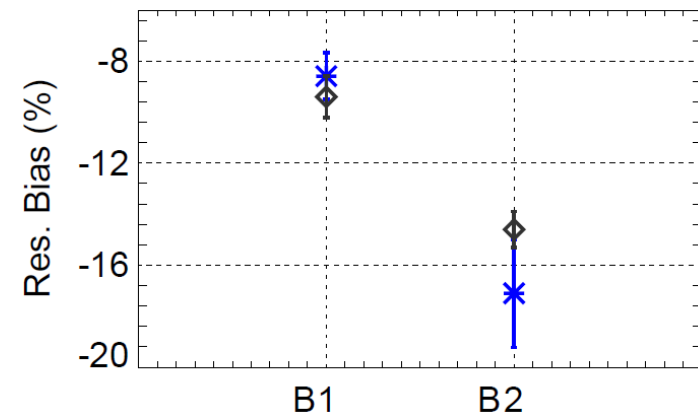
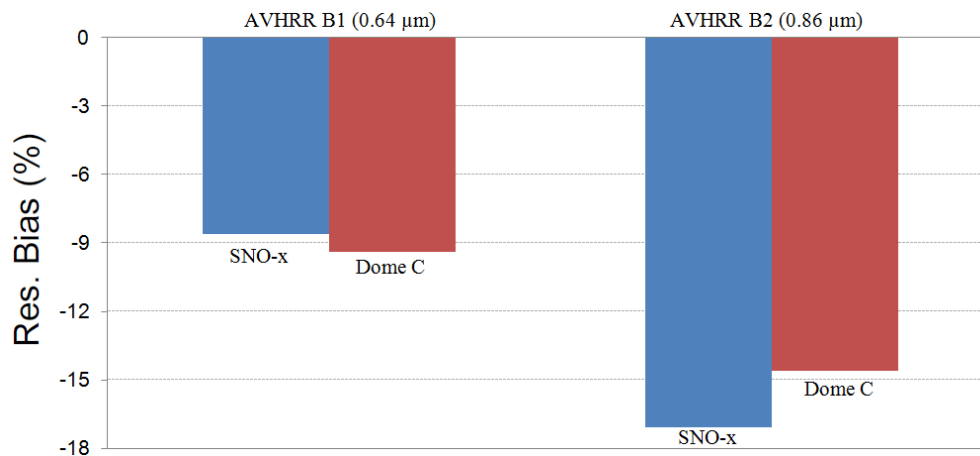
$$- \text{ESB} = \frac{(\text{Conv}_{\text{AVHRR}} - \text{Conv}_{\text{VIIRS}}) \times 100\%}{\text{Conv}_{\text{VIIRS}}} \quad \text{where, } \text{Conv}_i = \frac{\int \text{Hyp}_{\text{ref}}(\lambda) \cdot \text{SRE}_i(\lambda) \cdot d\lambda}{\int \text{SRE}_i(\lambda) \cdot d\lambda}$$



AVHRR	VIIRS	AVHRR Spectral Bias, (A-V)*100%/V	
		Libyan Desert	Dome C
B1 (0.64 μm)	M5	-9.7% ± 0.3%	-3.65% ± 0.4%
B2 (0.86 μm)	M7	-15.1% ± 2.3%	-7.9% ± 0.7%

Residual Bias of AVHRR

- Large bias for some VIIRS bands exists mainly due to the differences in spectral response functions of instruments.
- If the spectral characteristics of the sites are well characterized, the impact of spectral differences in inter-comparison can be accounted.
- **Residual Bias: Observed Bias** (measurements) – **ESB** (spectral differences)
- Residual bias over desert should agree with Dome C irrespective of the spectral differences.



AVHRR		VIIRS		Residual Bias	
Band	Wavelength (μm)	Band	Wavelength (μm)	African Desert	Dome C
1	0.58 – 0.68	M-5	0.662 - 0.682	-8.60% ± 0.91%	-9.4 ± 0.83%
2	0.725 – 1.0	M-7	0.846 - 0.885	-17.1 ± 2.12%	-14.6 ± 0.71%

Summary and Future Work

- SNO-x inter-comparison indicates relative degradation of AVHRR band 1 ($0.64 \mu\text{m}$) by 1.2% over the period of last two years.
- SNO-x suggests that AVHRR bias relative to VIIRS is $-8.6\% \pm 0.9\%$ for band 1 ($0.64 \mu\text{m}$) and $-17.1\% \pm 2.1\%$ for band 2 ($0.86 \mu\text{m}$).
- Larger bias for AVHRR B1 is believed to be due to calibration uncertainties. However, the large bias and large uncertainty for AVHRR band 2 is primarily due to the presence of water vapor absorption wavelength in its SRF.
- Radiometric bias estimated over Antarctica Dome C site agrees well with SNO-x to within 0.8% for AVHRR B1 and 2.5% for AVHRR B2.
- SNO inter-comparison over high latitude polar region indicates stable trends but with larger variability of more than 5% both for AVHRR B1 and B2.
- Large variability in SNO time series is mainly due to comparison over different target types in NH (such as snow, ocean, vegetation) and change in solar geometry during summer and winter solstice.
- The approach can be used to connect other AVHRR sensors back in time into same radiometric scale.

References

- Uprety, Sirish, Changyong Cao, Xiaoxiong Xiong, Slawomir Blonski, Aisheng Wu, Xi Shao 2013. “Radiometric Inter-comparison between Suomi NPP VIIRS and Aqua MODIS Reflective Solar Bands using Simultaneous Nadir Overpass in the Low Latitudes”. *Journal of Atmospheric and Oceanic Technology*, 30, pp:2720–2736.
- Cao Changyong, Frank DeLuccia, Xiaoxiong Xiong, Robert Wolfe, Fuzhong Weng (2013). “Early On-orbit Performance of the Visible Infrared 1 Imaging Radiometer Suite (VIIRS) onboard the Suomi National Polar-orbiting Partnership (S3 NPP) Satellite”, *IEEE Transaction on Geoscience and Remote Sensing*, Volume: 52, Issue: 2, pp: 1142 - 1156.
- Cao, Changyong, J. Xiong, S Blonski, Q Liu, S Uprety, X Shao, Y Bai, F Weng, 2013. "Suomi NPP VIIRS sensor data record verification, validation, and long-term performance monitoring". *Journal of Geophysical Research: Atmospheres*, 118 (20), 11,664-11,678.
- Cao, Changyong, Sirish Uprety, Jack Xiong, Aisheng Wu, Ping Jing, David Smith, Gyanesh Chander, Nigel Fox, and Stephen Ungar, 2010. "Establishing the Antarctic Dome C Community Reference Standard Site towards consistent Measurements from Earth Observation Satellites". *Canadian Journal of Remote Sensing*, 36:(5) , pp: 498-513.
- Uprety, Sirish, and Changyong Cao, 2012. “Radiometric and spectral characterization and comparison of the Antarctic Dome C and Sonoran Desert sites for the calibration and validation of visible and near-infrared radiometers”. *J. Appl. Remote Sens.* 6(1), 063541.
- Sirish Uprety, Changyong Cao, Slawomir Blonski, Xi Shao, 2013. "Evaluating radiometric consistency between Suomi NPP VIIRS and NOAA-19 AVHRR using extended simultaneous nadir overpass in the low latitudes". *Proc. of SPIE* Vol. 8866.
- Cao, C., M. Weinreb, and H. Xu, 2004. “Predicting Simultaneous Nadir Overpasses among Polar-Orbiting Meteorological Satellites for the Intersatellite Calibration of Radiometers”. *J. Atmos. Oceanic Technol.*, 21, 537–542.